Available online at www.sciencedirect.com

ScienceDirect

IFAC Papers Online CONFERENCE PAPER ARCHIVE

IFAC PapersOnLine 58-4 (2024) 437–442

Estimation of cornering stiffness using ultra-local model and LPV-based observer

Dániel Fényes, Tamás Hegedűs, Péter Gáspár

HUN-REN Institute for Computer Science and Control (SZTAKI), Kende u. 13-17 H-1111 Budapest, Hungary; E-mail: [daniel.fenyes,tamas.hegedus,peter.gaspar]@sztaki.hu
Department for Control of Transportationand Vehicle Systems, Budapest University of Technology and Economics, Stoczek u 2., H-1111 Budapest, Hungary. E-mail:[peter.gaspar]@kjk.bme.hu

Abstract: The paper presents an observer design method for estimating the slips and the cornering stiffness of autonomous road vehicles. As a first step, the dynamical one-wheeled bicycle model is reformulated to express directly the slips of the vehicle. In the second step, a polytopic model-based observer is designed which can deal with the variation of the scheduling parameters (longitudinal velocity, cornering stiffness). In order to eliminate the parameter uncertainty an ultra-local model is applied by which the cornering stiffness is estimated. The effectiveness and the operation of the proposed observer method are demonstrated through a complex scenario in the high-fidelity simulation software, CarMaker.

Keywords: ultra-local model, observer, lateral dynamics, cornering stiffness

1. INTRODUCTION AND MOTIVATION

One of the primary requirements for the widespread of autonomous or highly automated vehicles is the safe operation in all possible traffic situations. This covers several sub-problems, such as collision-free trajectory computation, decision-making, or control design. Mainly, the control design relies on the accurate model of the system, which involves several challenges due to the nonlinearities and parameter uncertainties of the considered system. In lateral vehicle control, one of the main difficulties is the estimation of the tire characteristics since it requires the accurate estimation of the side-slip angles and also the lateral forces. Moreover, during the operation of the system, the tire force characteristics can change or several effects highly influence the maximum lateral forces such as the tire pressure, the adhesion coefficient of the road or the temperature of the environment. However, an accurate tire model is essential for accurate trajectory tracking especially at high lateral acceleration maneuvers.

Although the tire modeling process can be carried out using force and accurate lateral velocity sensors, these solutions are not suitable for commercial use due to the high additional costs. Therefore, in recent years, several approaches have been developed to solve the problems regarding the estimation process of tire characteristics. In Wei et al. (2023) a physics-data-based approach is presented for the modeling process of the lateral dynamics, involving the unknown parameters of the vehicle, such as the cornering stiffness. The main advantage of the presented method is that it can capture the nonlinearities of the lateral dynamics, while no calibration or training process is needed. A method for lateral dynamics modeling can be found in Zhou et al. (2021), which combines the data-driven and physical model-based solutions. In the paper, the cornering stiffnesses are calculated using the neural network during the implementation, which makes the modeling process more accurate. Moreover, the tire characteristics can be approximated Boyali et al. (2021) using the Approximate Bayesian Computation method. The presented algorithm is tested on a double-lane change maneuver, during which the yaw-rate measurements are compared to the numerical solutions. Moreover, an iterative structure is proposed in Hsiao and Yang (2016) for both the tire stiffness and the road friction estimation using a modified tire model.

As mentioned, the lateral dynamics of the vehicle are influenced by nonlinear effects and parameter uncertainties, which must be taken into account to achieve a high-performance level during the estimation. These problems can be effectively handled by several methods such as the polytopic system-based approaches Perez-Estrada et al. (2018), or the robust $\mathcal{H}_\infty$-based solutions Jung et al. (2006). Although these methods are suitable to capture the nonlinearities or uncertainties, the maximum performance

⋆ The paper was funded by the National Research, Development and Innovation Office under OTKA Grant Agreement No. K 143599. The work of Daniel Fenyes was supported by the Janos Bolyai Research Scholarship of the Hungarian Academy of Sciences. The research was partially supported by the European Union within the framework of the National Laboratoryfor Autonomous Systems (RRF-2.3.1-21-2022-00002).

10.1016/j.ifacol.2024.07.257

level highly relies on the accuracy of the identified model of the system. Moreover, during the operation of the system, several parameters may change. A new approach has come up to effectively handle the nonlinearities and uncertainties, which was originally formulated for control problems and called the Ultra-Local Model-based control Fliess and Join (2013). The main idea behind this approach is to compute the Ultra-Local Model in every time step, which includes the unknown effects of the system. Using this, the performance level of the control algorithm can be increased. However, this approach has been augmented for estimation problems Al Younes et al. (2015).

In this paper, a parallel tire stiffness and side-slip angle estimation algorithm is proposed. The main contributions of the paper are:

(1) An LPV-based observer design for estimating the side-slips of front and rear axles using a transformed model of the classical dynamical bicycle model. The polytopic model considers the cornering stiffness and the longitudinal velocity as scheduling parameters.
(2) Estimation of the change in the cornering stiffness through an Ultra-Local Model-based algorithm. This serves two goals:
A. Using the corrected cornering stiffness the polytopic observer can provide a more accurate estimation from the estimated slips and the cornering stiffness
B. The tire characteristics can be built up and even online updated during the operation of the vehicle.

The rest of the paper consists of the following sections: The lateral model and its transformed version are presented in Section 2. The applied methods such as LPV-based observer design and the Ultra-Local Model (or Model-Free Control) technique are detailed in Section 3. The design steps of the combined method for the slip and cornering stiffness estimation problem are given in Section 4. Finally, a complex test scenario is presented in Section 5 using the high-fidelity vehicle dynamics simulation software, CarMaker.

2. MODELING OF LATERAL DYNAMICS

In this section, the modeling of the lateral dynamics of the vehicle is presented. The basis of the lateral model is the two-wheeled bicycle model, see Hahn et al. (2004). The original model has two state-variables: yaw-rate ($\dot{\psi}$) and the lateral velocity (v_y) or side-slip $\left(\beta = tan^{-1}\left(\frac{v_y}{v_x}\right)\right)$. This model implicitly contains the slips of the front and the rear axes (α_f, α_r) thus it makes the observer design process difficult.
In Balazs Nemeth (2016) a new formulation of the two-wheeled bicycle model is presented. The main advantage of it is that the state variables of the model are the slips of the front and rear axes, which makes it more suitable for an observer algorithm. In the rest of this section, the original and modified models are detailed and then the polytopic state-space presentation is formed, which will be the basis of the observer design.

2.1 Original bicycle model

The main idea behind the bicycle model is to replace the wheels on the front and rear axles with one wheel placed on the axis of symmetry of the vehicle. This approach neglects the roll and pitch dynamics and focuses only on the lateral dynamics of the vehicle.
The model consists of two equations: The first one describes the yaw motion while the second one is the lateral acceleration of the vehicle:

$$I_z\ddot{\psi} = \mathcal{F}_f(\alpha_f)l_f - \mathcal{F}_r(\alpha_r)l_r, \tag{1a}$$

$$mv_x(\dot{\psi} + \dot{\beta}) = \mathcal{F}_f(\alpha_f) + \mathcal{F}_r(\alpha_r). \tag{1b}$$

where I_z denotes the yaw-inertia, $\mathcal{F}_i(\alpha_i)$ $i \in [f, r]$ is the lateral forces on the front (f) and rear (r) axis as a function of the slips (α_f, α_r), l_f, l_r are geometric parameters, the mass of the vehicle is given by m and v_x is the longitudinal velocity.
The tire slips can be computed from the steering angle (δ), side-slip (β), yaw-rate $(\dot{\psi})$ and longitudinal velocity (v_x) using linearized equations:

$$\alpha_f = \delta - \beta - \frac{\dot{\psi}l_f}{v_x}, \tag{2a}$$

$$\alpha_r = -\beta + \frac{\dot{\psi}l_r}{v_x}. \tag{2b}$$

2.2 Model with slips as states

The states of the lateral model can be changed to tire slips by applying the following steps:
1. Reordering the equations (2) as:

$$\dot{\psi} = v_x\frac{\alpha_r - \alpha_f + \delta}{l_f + l_r}, \tag{3a}$$

$$\beta = -\frac{\alpha_f l_r + \alpha_r l_f - l_r\delta}{l_f + l_r}. \tag{3b}$$

Note that v_x is considered to be constant and it is handled later on as a scheduling parameter.
2. Computing the derivative of (3):

$$\ddot{\psi} = v_x\frac{\dot{\alpha}_r - \dot{\alpha}_f + \dot{\delta}}{l_f + l_r}, \tag{4a}$$

$$\dot{\beta} = -\frac{\dot{\alpha}_f l_r + \dot{\alpha}_r l_f - l_r\dot{\delta}}{l_f + l_r}. \tag{4b}$$

3. Subtracting Equations (1) from (4), the derivative of the slips (α_f,α_r) can be expressed as:

$$\dot{\alpha}_r - \dot{\alpha}_f = \frac{l_f + l_r}{I_z}(\mathcal{F}_f(\alpha_f)l_f - \mathcal{F}_r(\alpha_r)l_r) - \dot{\delta}, \tag{5a}$$

$$\dot{\alpha}_f l_r + \dot{\alpha}_r l_f = v_x(\alpha_r - \alpha_f) + v_x\delta + l_r\dot{\delta} - \frac{l_f + l_r}{mv_x}(\mathcal{F}_f(\alpha_f) + \mathcal{F}_r(\alpha_r)). \tag{5b}$$

As the last equation shows, the derivative of the steering angle is necessary for this model. The derivative of the steering can be approximated as $\dot{\delta} \cong max\left(\frac{|\dot{\delta}|}{|\delta|}\right)\delta = \varphi\delta$, more details can be seen in Balazs Nemeth (2016).

2.3 State-space representation of the modified model

The presented lateral model is transformed into a polytopic state-space representation. One of the main sources

of the nonlinearities of the lateral dynamics comes from the slip-tire force characteristics. This function can be linearized as $\mathcal{F}_i = C_i\alpha_i$. C_i represents the cornering stiffness of the tire. The cornering stiffness can change in a wide range during the operation of the vehicle thus it is handled as a scheduling parameter, which leads to the following state space representation:

$$\dot{x}_v = A_v(\rho)x_v + B_v(\rho)u_v, \tag{6a}$$
$$y_v = c_v^T(\rho)x_v, \tag{6b}$$
$$\begin{bmatrix}\dot{\alpha}_f\\ \dot{\alpha}_r\end{bmatrix} = \underbrace{\begin{bmatrix}a_{11}(\rho) & a_{12}(\rho)\\ a_{21}(\rho) & a_{22}(\rho)\end{bmatrix}}_{A_v(\rho)}\begin{bmatrix}\alpha_f\\ \alpha_r\end{bmatrix} + \underbrace{\begin{bmatrix}b_1(\rho)\\ b_2(\rho)\end{bmatrix}}_{B_v(\rho)}\delta, \tag{6c}$$
$$ma_y = mv_x(\dot{\beta}+\dot{\psi}) = [C_f(t)\ C_r(t)]\begin{bmatrix}\alpha_f\\ \alpha_r\end{bmatrix}. \tag{6d}$$

where the output of the system is the lateral force ($y_v = ma_y = mv_x(\dot{\beta}+\dot{\psi})$), and scheduling vector consists of the following variables: $\rho = [C_f(t), C_r(t), v_x(t)]$.
Other parameters of the state-matrices are:

$$a_{11}(\rho) = -\frac{C_f(t)l_f^2}{I_z v_x} - \frac{v_x(t)}{l_f+l_r} - \frac{C_f(t)}{mv_x(t)}, \tag{7a}$$
$$a_{12}(\rho) = \frac{C_r(t)l_f l_r}{I_z v_x(t)} + \frac{v_x(t)}{l_f+l_r} - \frac{C_r(t)}{mv_x(t)}, \tag{7b}$$
$$a_{21}(\rho) = \frac{C_f(t)l_r l_f}{I_z v_x(t)} - \frac{v_x(t)}{l_f+l_r} - \frac{C_f(t)}{mv_x(t)}, \tag{7c}$$
$$a_{22}(\rho) = -\frac{C_r(t)l_r^2}{I_z v_x(t)} + \frac{v_x(t)}{l_f+l_r} - \frac{C_r(t)}{mv_x(t)}, \tag{7d}$$
$$b_1(\rho) = \frac{v_x(t)}{l_f+l_r} + \varphi, \tag{7e}$$
$$b_2(\rho) = \frac{v_x(t)}{l_f+l_r}. \tag{7f}$$

3. APPLIED METHODS FOR OBSERVER DESIGN

In this section, the applied methods for observer design are presented. Linear Parameter Varying (LPV) framework-based observer design is used to estimate the slips of vehicle (α_f, α_r), while the non-measurable scheduling parameters (Cornering stiffness C_f, C_r) are continuously computed by an Ultra-Local Model and the longitudinal velocity can be measured.

3.1 Ultra-Local Model and Model-Free Control

The Model-Free Control strategy is a relatively new control technique, which was proposed by Fliess and Join (2013, 2009); d'Andrea Novel et al. (2010). As advertised, this method does not require a model of the control system but it uses a so-called Ultra-Local Model to compensate the nonlinearities/unknown dynamics of the system.
The basis of this algorithm is a 'phenomenological' model, which is given as:

$$y^{(\nu)} = F + \alpha u, \tag{8}$$

where F denotes the Ultra-Local Model, α is a free tuning parameter of this technique, y is the measured output of the system, ν represents the derivative order, u is the control input. The Ultra-Local Model can be computed as:

$$F = y^{(\nu)} - \alpha u \tag{9}$$

The aim of the controller is to guarantee the zero steady-state error in terms of ν^{th} derivative of the error signal, as:

$$e^{(\nu)} = y^{(\nu)} - y_{ref}^{(\nu)} = F + \alpha u - y_{ref}^{(\nu)} \tag{10}$$

where y_{ref} is the reference signal. Moreover, $e^{(\nu)} = 0$ is guaranteed by the open loop control:

$$u = \frac{-F + y_{ref}^{(\nu)}}{\alpha} \tag{11}$$

However, it cannot guarantee the zero steady-state error in terms of the error signal ($e = y_{ref} - y$) thus an additional controller ($C(s)$) is applied:

$$u_{\text{ulm}} = \frac{-F + y_{ref}^{(\nu)} + C(s)e}{\alpha} \tag{12}$$

the structure of $C(s)$ is not prescribed or restricted it can be freely chosen, such as PID Fliess and Join (2009) or LQR Younes et al. (2016).
Note that this technique will be used to detect the change in the cornering stiffness. Since it is used only for observation not for intervention the additional controller is set to zero ($C(s) = 0$). The application of the Ultra-Local Model for this specific problem can be found in Section IV.

3.2 LPV-based observer design

As presented in Section 2, the model of the lateral dynamics contains three time-variant parameters or scheduling variables, namely: longitudinal velocity (v_x) and cornering stiffness (C_f, C_r). Therefore an LPV framework-based technique is used to design an observer, which can handle these time-dependent variables. In the rest of this subsection, a brief introduction is given to LPV system-based observer design.

Considering a state-space representation of a system with time-variant state matrices, see Tóth (2010):

$$\dot{x} = A(\rho)x + B(\rho)u \tag{13a}$$
$$y = c^T(\rho)x + D(\rho)\omega \tag{13b}$$

where the time variant state matrices are: $A(\rho)$, $B(\rho)$, $c^T(\rho)$, $D(\rho)$, x is the states-vector of the system, u denotes the control input, y is the output while ω is the external disturbance. The observer aims to estimate the nonmeasurable states of the system, which leads to a minimization problem:

$$e = x - \hat{x}, \qquad |e| \to min! \tag{14}$$

where $\hat{x}$ is the estimated state-vector, which can be computed as Kang and Kim (2020):

$$\dot{\hat{x}} = A(\rho)\hat{x} + B(\rho)u + L(\rho)(y - c^T(\rho)\hat{x}), \tag{15}$$

where $L(\rho)$ is the observer gain vector, which must depend on the scheduling variables (ρ).

The following LPV model can built up by using (13) and (15):

$$T(\rho)_{z_e,\omega}\begin{cases}\dot{e} = (A(\rho) + L(\rho)c^T(\rho))e + L(\rho)D(\rho)\omega,\\ z_e = C(\rho)e,\end{cases} \tag{16}$$

where z_e is a vector, which contains the predefined performances. The designed observer must guarantee the predefined performances while attenuating the effect of the external disturbances . This can be achieved by minimizing the $\mathcal{L}_2$ norm form the disturbances to the performances :

$$\inf_{L(\rho,y_m)} \sup_{\rho\in\varrho} \sup_{\substack{\|\omega\|_2\neq 0,\\ \omega\in\mathcal{L}_2}} \frac{\|z_e\|_2}{\|\omega\|_2}, \tag{17}$$

where y_m contains the measured signals and ϱ covers the range of the scheduling variable. This optimization problem can be solved by using LMI or Lyapunov function-based solutions, see Zemouche et al. (2016), Briat et al. (2011).

4. OBSERVER DESIGN

In the previous sections, the models and the methods that are used in the observer design have been presented. In this section the main steps of the design process are detailed, specifically for the slip estimation problem.

(1) Determination of the nominal model, which is used for the polytopic observer design, see Section 2. The presented model is in a continuous form, however, it must be discretized before designing the observer, see Tóth (2010). The sampling time is set to $T_s = 0.01s$.
(2) Design the LPV observer, as presented in Section 3.
(3) Selection of the output and the derivative order for the Ultra-Local Model. In this paper, $y_{ulm} = \dot{\psi}$ and $\nu = 1$ are selected since $\dot{\psi}$ is easily measurable and independent from the LPV observer.
(4) Selection of derivative algorithm, ALIEN filter is a frequently used technique for computing a derivative of a noisy, measured signal, therefore it is suitable for this application. ALIEN filter algorithm is detailed in Polack et al. (2019).
(5) Tuning of parameter α. In the case of lateral control a technique has been presented in Hegedus et al. (2022), which is applicable to the observer design as well.
(6) Determination of the reference signal and its derivative and the computation of the cornering stiffness, see Subsection 4.1.
(7) Interconnection of the whole algorithm.

The structure of the whole algorithm is illustrated in Figure 1.

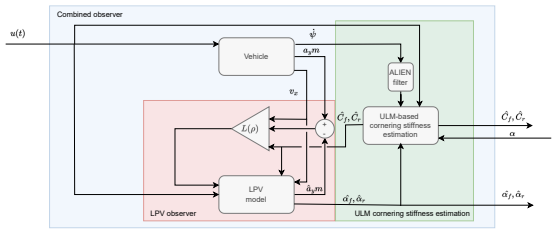

Fig. 1. Schematic structure of the observer

4.1 Computation of the reference signal and cornering stiffness

In this subsection, the computation of the reference signal and the cornering stiffness are presented. As mentioned the output for the Ultra-Local Model is the yaw-rate $y_{ulm} = \dot{\psi}$ and the derivative order is set $\nu = 1$. The Ultra-Local Model can be approximated as:

$$\hat{F} = \dot{\hat{\psi}} - \alpha\delta \tag{18}$$

Note that $u = \delta$, see: (6c). $\ddot{\psi}(t)$ can be computed using the states and the dynamic model of the vehicle (1):

$$\dot{\hat{\psi}}(t) = \frac{\hat{\alpha}_f(t)C_f(t)l_f}{I_z} - \frac{\hat{\alpha}_r(t)C_r(t)l_r}{I_z}. \tag{19}$$

Using the Ultra-Local Model, the additional control input can be calculated as:

$$u_{ulm} = \frac{-\hat{F} + \ddot{\psi}_{ref}}{\alpha}, \tag{20}$$

where the derivative of the reference signal can be determined using the ALIEN filter and the measured yaw-rate ($\dot{\psi}$). Since the main role of the Ultra-Local Model-based part is to eliminate the effect of nonlinearities or unmodelled dynamics of the system,in this application, the Ultra-Local Model is used to compensate the tire stiffness. Let's consider the dynamics of LPV observer without the Ultra-Local Model:

$$\dot{\hat{x}}_v = A_v(\rho)\hat{x}_v + B_v(\rho)u + L(\rho)(y_v - c_v^T(\rho)\hat{x}_v) \tag{21}$$

where $\hat{x}_v = [\hat{\alpha}_f, \hat{\alpha}_r]$
The effect of the Ultra-Local Model, appears as an additional control input (u_{ulm}) through vector B_v. Moreover, this additional control input generates a change in the derivatives of the states ($\Delta\dot{\hat{x}}_v$), which can be written as:

$$\dot{\hat{x}}_v + \Delta\dot{\hat{x}}_v = A_v(\rho)\hat{x} + B_v(\rho)u + L(\rho)(y_v - c_v^T(\rho)\hat{x}) + \\ + B(\rho)u_{ulm} \tag{22}$$

Finally, subtracting (21) from (22):

$$\Delta\dot{\hat{x}}_v = B(\rho)u_{ulm}. \tag{23}$$

The effect of $B(\rho)u_{ulm}$ will be transformed into a change in the cornering stiffness (ΔC_i) using the following way: Assuming that all other parameters (m, l_f, l_r, I_z) are known or the effects of their change on the lateral dynamics are negligible to the effect of the change in the cornering stiffness. The effect of the Ultra-Local Model is expressed as a change in the cornering stiffness.

In the first step, the state matrix (A_v, see: (6c)) can be divided into two main parts:

$$A_v = \underbrace{\begin{bmatrix} -\frac{C_f l_f^2}{I_z v_x} - \frac{C_f}{m v_x} & \frac{C_r l_f l_r}{I_z v_x} - \frac{C_r}{m v_x} \\ \frac{C_f l_r l_f}{I_z v_x} - \frac{C_f}{m v_x} & \frac{C_r l_r^2}{I_z v_x} - \frac{C_r}{m v_x} \end{bmatrix}}_{A_{v,1}} + \underbrace{\begin{bmatrix} -\frac{v_x}{l_f+l_r} & \frac{v_x}{l_r+l_f} \\ -\frac{v_x}{l_f+l_r} & \frac{v_x}{l_f+l_r} \end{bmatrix}}_{A_{v,2}} \tag{24}$$

For the sake of simplicity (t) and (ρ) are neglected. $A_{v,1}$ contains that parts of matrix A_v, which are linked to the cornering stiffness while elements of $A_{v,2}$ are not related to them.
In the second step, C_f, C_r can be extracted from $A_{v,1}$ as:

$$A_{v,1} = \underbrace{\begin{bmatrix} -\frac{l_f^2}{I_z v_x} - \frac{1}{m v_x} & \frac{l_f l_r}{I_z v_x} - \frac{1}{m v_x} \\ \frac{l_r l_f}{I_z v_x} - \frac{1}{m v_x} & -\frac{l_r^2}{I_z v_x} - \frac{1}{m v_x} \end{bmatrix}}_{A_{v,1,1}} \underbrace{\begin{bmatrix} C_f & 0 \\ 0 & C_r \end{bmatrix}}_{C_m} \tag{25}$$

It has been mentioned that the changes in the other parameters of the vehicle can be neglected alongside the change in tire stiffness. Therefore, the goal is to change the stiffness values to suppress the deviation between the measured and estimated values. This means, that the change of the tire stiffness ($\Delta C_f, \Delta C_r$) are computed using (23), (25):

$$\Delta\dot{\hat{x}}_v = A_{v,1,1}(C_{\Delta m}\hat{x}) \tag{26}$$

where $C_{\Delta m} = \begin{bmatrix} \Delta C_f & 0 \\ 0 & \Delta C_r \end{bmatrix}$. The change in the cornering stiffness can be computed by inverting matrix $A_{v,1,1}$ as:

$$\begin{bmatrix} -\frac{l_f^2}{I_z v_x} - \frac{1}{m v_x} & \frac{l_f l_r}{I_z v_x} - \frac{1}{m v_x} \\ \frac{l_r l_f}{I_z v_x} - \frac{1}{m v_x} & -\frac{l_r^2}{I_z v_x} - \frac{1}{m v_x} \end{bmatrix}^{-1} \begin{bmatrix} \frac{v_x}{l_f + l_r} + \varphi \\ \frac{v_x}{l_f + l_r} \end{bmatrix} u_{ulm} = \\ = \begin{bmatrix} \Delta C_f \hat{\alpha}_f \\ \Delta C_r \hat{\alpha}_r \end{bmatrix} \tag{27}$$

Finally, the updated cornering stiffness are:

$$\hat{C}_f(t) = \hat{C}_f(t-1) + \Delta\hat{C}_f(t), \tag{28}$$

$$\hat{C}_r(t) = \hat{C}_r(t-1) + \Delta\hat{C}_r(t). \tag{29}$$

5. SIMULATION RESULTS

In this section, a comprehensive simulation example is presented to show the operation and the effectiveness of the proposed estimation algorithm. The algorithm is implemented in MATLAB/Simulink environment and the dynamics of the vehicle is simulated by the high-fidelity simulation software, CarMaker. In the test scenario, a Tesla Model S is used, the main parameters of the car and the algorithm can be found in Table 1.

m	2100 (kg)
l_f, lr	1.5, 1.5 (m)
I_z	3900 (kgm^2)
ϕ	0.4 $\frac{1}{s}$
T_s	0.01s

Table 1. Parameters of the test vehicle

The vehicle is driven along a section of F1 track Hungaroring, which contains sharp bends, where the vehicle can reach the nonlinear zone of the tire characteristics, see Figure 2. The velocity profile is illustrated in Figure 3. The maximum of the longitudinal velocity is set to $70km/h$, which is reduced at a sharp bend. The test scenario is performed two times. In the first run, the proposed combined observer is used, while in the second one, the LPV observed is applied with fixed cornering stiffness ($C_f = 120000N/rad, C_r = 1200000N/rad$).

Figure 4 shows the lateral acceleration of the vehicle during the test scenario. As it can be seen the maximal value of it is around $8m/s^2$, which indicates that the vehicle is close to its physical limits. The steering angle is shown in Figure 5(a). The maximum of it is around $0.2rad$, which is a high value to generate high slip angles. In Figure 5(b) the yaw-rate of the vehicle can be seen. As it can be seen it covers a wide range $\dot{\psi} \in [-0.63, 0.38]rad/s$

The estimated and the measured side-slips are depicted in Figure 6. In case of the front slip, the proposed algorithm

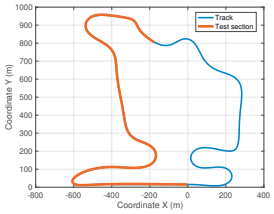

Fig. 2. Selected section of track

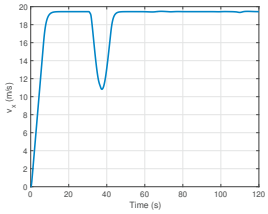

Fig. 3. Longitudinal velocity

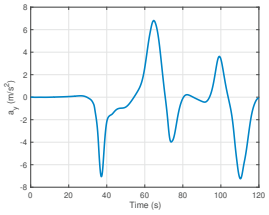

Fig. 4. Lateral acceleration

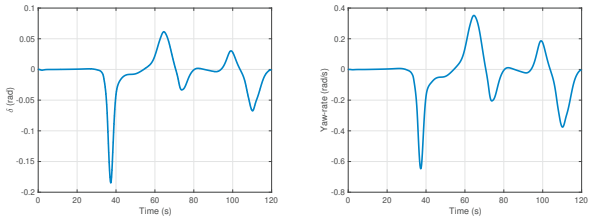

(a) Steering angle (b) Yaw-rate

Fig. 5. Steering angle and yaw-rate

provides slightly better results because the steering angle is measured, which is an influential component of the front slip. As it can be seen the estimation is accurate during the whole scenario, maximal error is $0.01rad$ at the peak. The average error is around $0.001rad$. The pure LPV-based observer provide worse result in both cases, the maximum error is around $0.015rad$.

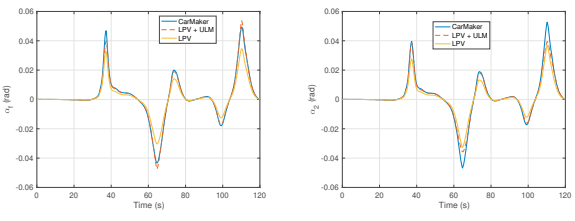

(a) Front slip (b) Rear slip

Fig. 6. Slips at front and rear axes

Figures 7 illustrate the estimated and the measured cornering stiffness of the vehicle. The largest change in the

cornering stiffness is more than $> 33\%$, which means that the vehicle reaches the nonlinear segment of the tire-slip characteristics. Although the estimation is accurate during the whole test scenario, between $80-105s$ a small deviation can be observed. The reason behind this phenomenon is that the slips are relatively low in this time range and, in parallel, the lateral forces are also low. Without enough excitation, the estimation algorithm cannot provide accurate results, which is a natural limit of all estimation algorithms.

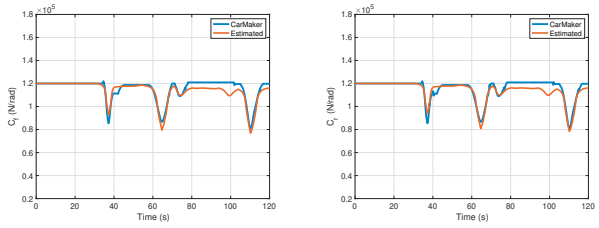

(a) Cornering stiffness of front (b) Cornering stiffness of rear

Fig. 7. Cornering stiffness

Finally, the tire characteristics are built up using the slips and the cornering stiffness, see in Figure 8. As it can be seen the tire characteristics are recovered with high accuracy without any expensive equipment or additional signals.

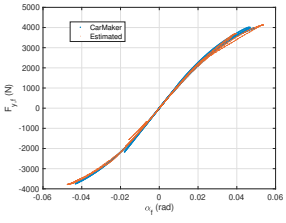

Fig. 8. Lateral forces and slips

6. CONCLUSION

In the paper, a novel slip and cornering stiffness estimation algorithm has been proposed. The slip estimation was based on the LPV paradigm, while the estimation of the cornering stiffness was based on an Ultra-Local Model. The combination of the two methods has increased the performance level and the accuracy of the estimation algorithm using available, measurable signals such as: lateral acceleration (a_y) and yaw-rate ($\dot{\psi}$). The proposed combined method has been implemented and tested in the simulation software, CarMaker and compared to a conventional LPV solution.

REFERENCES

Al Younes, Y., Noura, H., Muflehi, M., Rabhi, A., and El Hajjaji, A. (2015). Model-free observer for state estimation applied to a quadrotor. In *2015 International Conference on Unmanned Aircraft Systems (ICUAS)*, 1378–1384. doi: 10.1109/ICUAS.2015.7152433.

Balazs Nemeth, Peter Gaspar, T.P. (2016). Nonlinear analysis of vehicle control actuations based on controlled invariant sets. *International Journal of Applied Mathematics and Computer Science*, 26(1), 31–43. URL `http://eudml.org/doc/276550`.

Boyali, A., Thompson, S., and Wong, D.R. (2021). Identification of vehicle dynamics parameters using simulation-based inference.

Briat, C., Sename, O., and Lafay, J.F. (2011). Design of lpv observers for lpv time-delay systems: an algebraic approach. *International Journal of Control*, 84(9), 1533–1542. doi:10.1080/00207179.2011.611950. URL `https://doi.org/10.1080/00207179.2011.611950`.

Camila Le?o Pereira, R.T.d.C.N. and Loiola, B.R. (2021). Cornering stiffness estimation using levenberg?marquardt approach. *Inverse Problems in Science and Engineering*, 29(12), 2207–2238.

d'Andrea Novel, B., Fliess, M., Join, C., Mounier, H., and Steux, B. (2010). A mathematical explanation via 'intelligent' PID controllers of the strange ubiquity of pids. *Proc. 18th Mediterranean Conference on Control and Automation*, 395–400.

Fliess, M. and Join, C. (2009). Model-free control and intelligent PID controllers: Towards a possible trivialization of nonlinear control? *Proc. 15th IFAC Symposium on System Identification, Saint-Malo, France*, 42, 1531–1550.

Fliess, M. and Join, C. (2013). Model-free control. *International Journal of Control*, 86(12), 2228–2252.

Guo, H., Cao, D., Chen, H., Lv, C., Wang, H., and Yang, S. (2018). Vehicle dynamic state estimation: state of the art schemes and perspectives. *IEEE/CAA Journal of Automatica Sinica*, 5(2), 418–431. doi:10.1109/JAS.2017.7510811.

Hahn, J., Rajamani, R., You, S., and Lee, K. (2004). Real-time identification of road-bank angle using differential GPS. *IEEE Transactions on Control Systems Technology*, 12, 589–599.

Hegedus, T., Fenyes, D., Nemeth, B., Szabo, Z., and Gaspar, P. (2022). Design of model free control with tuning method on ultra-local model for lateral vehicle control purposes. In *2022 American Control Conference*.

Hsiao, T. and Yang, J.W. (2016). Iterative estimation of the tire-road friction coefficient and tire stiffness of each driving wheel. In *2016 American Control Conference (ACC)*, 7573–7578. doi: 10.1109/ACC.2016.7526869.

Jung, J., Huh, K., Fathy, H., and Stein, J. (2006). Optimal robust adaptive observer design for a class of nonlinear systems via an h-infinity approach. 6 pp.–.

Kang, C.M. and Kim, W. (2020). Linear parameter varying observer for lane estimation using cylinder domain in vehicles. *IEEE Transactions on Intelligent Transportation Systems*, 1–10. doi: 10.1109/TITS.2020.3000957.

Perez-Estrada, A.J., Osorio-Gordillo, G.L., Darouach, M., Alma, M., and Olivares-Peregrino, V.H. (2018). Generalized dynamic observers for quasi-lpv systems with unmeasurable scheduling functions. *International Journal of Robust and Nonlinear Control*, 28(17), 5262–5278.

Polack, P., Delprat, S., and dAndrea Novel, B. (2019). Brake and velocity model-free control on an actual vehicle. *Control Engineering Practice*, 92, 1–8.

Tóth, R. (2010). *Discretization of LPV Systems*, 143–169. Springer Berlin Heidelberg, Berlin, Heidelberg.

Wei, W., Yin, G., and He, T. (2023). Physics-informed data-based lpv modeling and validations of lateral vehicle dynamics. *IEEE Transactions on Intelligent Vehicles*, 1–10. doi: 10.1109/TIV.2023.3303013.

Younes, Y.A., Drak, A., Noura, H., Rabhi, A., and El Hajjaji, A. (2016). Robust Model-Free Control Applied to a Quadrotor UAV. *Journal of Intelligent and Robotic Systems*, 84, 37 – 52.

Zemouche, A., Zerrougui, M., Boulkroune, B., Rajamani, R., and Zasadzinski, M. (2016). A new lmi observer-based controller design method for discrete-time lpv systems with uncertain parameters. 2802–2807.

Zhou, Z., Wang, Y., Ji, Q., Wellmann, D., Zeng, Y., and Yin, C. (2021). A hybrid lateral dynamics model combining data-driven and physical models for vehicle control applications. *IFAC-PapersOnLine*, 54(20), 617–623. Modeling, Estimation and Control Conference MECC 2021.

Zhu, Z., Tang, X., Qin, Y., Huang, Y., and Hashemi, E. (2023). A survey of lateral stability criterion and control application for autonomous vehicles. *IEEE Transactions on Intelligent Transportation Systems*, 24(10), 10382–10399. doi: 10.1109/TITS.2023.3280200.